Published in final edited form as:
Magn Reson Med. 2008 October ; 60(4): 987–996. doi:10.1002/mrm.21759.

Anesthetic Effects on Regional CBF, BOLD, and the Coupling Between Task-Induced Changes in CBF and BOLD: An fMRI Study in Normal Human Subjects

Maolin Qiu[1,*], **Ramachandran Ramani**[2], **Michael Swetye**[1], **Nallakkandi Rajeevan**[1], and **R. Todd Constable**[1,3,4]

[1]Department of Diagnostic Radiology, Yale University School of Medicine, New Haven, Connecticut.

[2]Department of Anesthesiology, Yale University School of Medicine, New Haven, Connecticut.

[3]Department of Biomedical Engineering, Yale University School of Medicine, New Haven, Connecticut.

[4]Department of Neurosurgery, Yale University School of Medicine, New Haven, Connecticut.

Abstract

Functional MR imaging was performed in sixteen healthy human subjects measuring both regional cerebral blood flow (CBF) and blood oxygen level dependent (BOLD) signal when visual and auditory stimuli were presented to subjects in the presence or absence of anesthesia. During anesthesia, 0.25 mean alveolar concentration (MAC) sevoflurane was administrated. We found that low-dose sevoflurane decreased the task-induced changes in both BOLD and CBF. Within the visual and auditory regions of interest inspected, both baseline CBF and the task-induced changes in CBF decreased significantly during anesthesia. Low-dose sevoflurane significantly altered the task-induced CBF-BOLD coupling; for a unit change of CBF, a larger change in BOLD was observed in the anesthesia condition than in the anesthesia-free condition. Low-dose sevoflurane was also found to have significant impact on the spatial nonuniformity of the task-induced coupling. The alteration of task-induced CBF-BOLD coupling by low-dose sevoflurane introduces ambiguity to the direct interpretation of functional MRI (fMRI) data based on only one of the indirect measures—CBF or BOLD. Our observations also indicate that the manipulation of the brain with an anesthetic agent complicates the model-based quantitative interpretation of fMRI data, in which the relative task-induced changes in oxidative metabolism are calculated by means of a calibrated model given the relative changes in the indirect vascular measures, usually CBF and BOLD.

Keywords

cerebral blood flow; blood oxygen level dependent signal; anesthesia; sevoflurane; minimum alveolar concentration

Under normal circumstances increased focal neuronal activity is associated with a large increase in regional cerebral blood flow (CBF) along with small changes in oxygen consumption (1,2). Changes in oxygen supply, oxygen consumption, and vascular occupancy result in a change in the concentration of deoxyhemoglobin [dHb] in blood. Because dHb is

*Correspondence to: Maolin Qiu, Yale University School of Medicine, Department of Diagnostic Radiology, MRRC, The Anlyan Center, N127, 300 Cedar Street, New Haven, CT 06520−2048. E-mail: E-mail: maolin.qiu@yale.edu.

paramagnetic (3,4), local magnetization fluctuations could be observed due to changes in [dHb], which is the physiological origin of the widely used blood oxygenation level dependent (BOLD) contrast in functional MRI (fMRI). These empirical coupling relationships, in terms of the supply and consumption of oxygen, are generally assumed to be unchanged in normal human subjects under most circumstances, thus allowing BOLD and CBF to be used as indices of neuronal activity. Understanding these coupling relationships is important in all studies, but there are two categories of studies in which a clear understanding is critical because the relationship may be altered: (i) imaging studies performed in the presence of an anesthetic. Functional imaging studies of animals are performed routinely using anesthesia to immobilize the animal. Anesthetics are also used increasingly in animal and human studies, both to understand the pharmacology of anesthetic agents and to investigate the impact of such agents on brain function and the signature of that function (5–9); (ii) imaging studies performed in the presence of other medications. In a resent study focusing on the confounding effects of anesthesia on functional activation (10), it was showed that a greater BOLD response was observed during α-chloralose anesthesia relative to halothane for a fixed stimulus, and the BOLD response varied substantially in spatial extent and magnitude over time, suggesting that the varied sensitivity of different brain regions to the effects of anesthesia may bias fMRI studies that are dependent on constant coupling between the vascular and metabolic components.

Sevoflurane was used in this study to depress the neuronal activity of the brain. Anesthetic-sensitive ion-channel proteins that control neuronal excitability are the most likely channels that an anesthetic acts on. Research on these proteins has revealed that γ-aminobutyric acid type A ($GABA_A$) receptors are likely involved in the molecular actions of sevoflurane (11–17). It may also act by inhibiting excitatory ion channels such as neuronal nicotinic and glutamate receptors (12,18–22). The action of a volatile agent on neurotransmitter receptors is dominant, while it also affects the release of neurotransmitters. Ion channels are involved in a wide variety of biological processes that are responsible for rapid changes in cells, such as cardiac, skeletal, and smooth muscle contraction, epithelial transport of nutrients and ions, T-cell activation and pancreatic beta-cell insulin release. The direct action of an anesthetic agent on the receptors of vascular smooth muscle will cause vascular contraction or dilation. In fMRI studies involving anesthetic agents, the brain vasculature responds in part to the task stimulation and in part to the anesthetic, which complicates fMRI data interpretation or data modeling. A key issue in examining the effects of anesthetic agents on the brain is to dissociate the purely vascular effects from neuronal excitability effects.

We hypothesize that sevoflurane significantly alters the task-induced changes in CBF and BOLD, baseline CBF, and the coupling of CBF and BOLD even at low dose. This work examines these relationships under conditions of pharmacological manipulation of normal human brain using a pulsed-ASL and BOLD imaging sequence. Sevoflurane, at 0.25 MAC, was used to investigate in humans, how task-induced changes, baseline CBF, and more importantly, the CBF-BOLD coupling can be altered in different cortical regions. Based upon our observation and data simulation, we examined closely the possible parameters changes in the fMRI quantitative model, and suggest more parameters of the model be calibrated, which will have important implications for fMRI practice and quantitative fMRI when a drug is involved.

MATERIALS AND METHODS

Subjects and Anesthetic Administration

Sixteen healthy consenting subjects (American Society of Anesthesiologists, physical status class I) 19- to 30-year-old were administered inhalational 0.25 MAC end-tidal sevoflurane. Subjects on psychoactive drugs or any centrally acting medication were excluded. Subjects

with a history of renal disease and those with potentially difficult airway were also excluded. All patients fasted for 8 h before the study. After passing the physical and medical history examination, subjects proceeded to the magnetic resonance research center (MRRC) where they were screened for ferromagnetic materials and then connected to standard ASA (American Society of Anesthesiologists) monitors. An intravenous infusion line was started with a 22G cannula for maintenance infusion (lactated ringer at 100 mL/h). Subjects were moved into the magnet with the monitors and intravenous infusion line in place. Anesthesia was induced and maintained with oxygen (5 liters) and sevoflurane 0.5% (0.25 MAC) administered through a semi-closed circuit and a facemask. The facemask was held in place with head straps. During anesthesia of 0.25 MAC sevoflurane, subjects were able to talk and respond to questions. ECG, noninvasive blood pressure, oxygen saturation, end-tidal carbon dioxide, and end-tidal sevoflurane concentration were monitored continuously throughout the study. The monitors used in this study are serviced and calibrated every 6 months, as recommended by the manufacturer, OHMEDA (Madison, WI).

Stimulation

Visual stimulation consisted of an 8 Hz reverse-flashing, full-field black and white checkerboard (shown as an inset in Fig. 3a). The horizontal and vertical extents were approximately 16 and 12 degrees, respectively. During rest intervals subjects fixated on a white plus sign (+) presented against a black background. The auditory stimulus consisted of randomly presented pure tones and a white-noise sound burst, presented through MR compatible headphones. The tones were played out at different frequencies (including 400, 600, 800, 1000, 1500, 2000, and 3000 Hz) in randomized order in a block design experiment. The duration of each tone was 250 ms with an ISI of 250 ms and the sound pressure level of the auditory stimulus was 95 dB, with attenuation by the ear inserts of 15 to 20 dB; this was determined in a pilot study and kept constant for all subjects. The auditory and visual stimuli were presented simultaneously in 4 cycles of 30-s blocks, alternating with 30-s periods of rest; these clusters started and ended with resting periods. Clinical practice and our pilot studies indicated that the end-tidal sevoflurane concentration reached a steady-state approximately 9 minutes after the induction of sevoflurane. Based on ECG readings, it took approximately 9 minutes for the subjects to recover after the withdrawal of the agent. The subject was positioned once at the beginning of the experiment; head straps and pads were used to help control head motion during the experiment. Two anesthesia sessions were interleaved with 3 anesthesia-free sessions. During each session, the stimulation procedure was repeated three times. Perfusion-weighted and BOLD-weighted MRI data were collected during all sessions.

Regional CBF and BOLD Measurements

Imaging was performed on a 3 Tesla (T) whole-body scanner Trio (Siemens Medical Systems, Erlangen, Germany) with a circularly polarized head coil. Pulsed arterial spin labeling imaging was performed to measure regional CBF and BOLD in the presence of auditory/visual stimuli in the anesthesia-free and anesthesia conditions with a modified EPISTAR QUIPSS ASL sequence (23,24). This involved applying a train of thin-slice saturation pulses at TI_1=700 ms after the radiofrequency (RF) inversion pulse so as to control the bolus delivery and suppress the intravascular signal from large vessels (25). A slab-selective hyper-secant RF inversion pulse was used for labeling the arterial blood water. The RF pulse was applied to a slab 20 mm inferior to the imaging slab. As a control, the same RF pulse was applied to a slab 20 mm superior to the imaging slab. Interleaved labeling and control images were acquired using a gradient echo-planar imaging (EPI) sequence, followed by a recovery time allowing arterial blood to be refreshed.

The ASL acquisition parameters were: field of view = 256 × 256 mm^2; matrix = 64 × 64; bandwidth = 2056 Hz/pixel; slice thickness = 8 mm; inter-slice spacing = 2 mm. Ten *AC-PC*

aligned slices were acquired from inferior to superior in an ascending order to cover most of the cortex. Acquisition of each slice took approximately 60 ms. The repetition time was *TR* = 3000 ms; the echo time was *TE* = 26 ms, and the delay time *TD* within each *TR* was adjusted to maximum, which was 900 ms. During each EPI acquisition, fat was suppressed and phase-correction was performed. A bipolar gradient of encoding velocity V_{enc} = 20 mm/s was applied to the imaging slices for intra-vascular signal suppression.

To get the absolute values for regional CBF, 40 proton density weighted images were acquired with the same perfusion sequence, except for the following changes: *TR* = 10,000 ms; *TD* = 0 ms; and within each *TR*, *TI* was adjusted to 7900 ms. Mapping for the apparent longitudinal relaxation time T_{1app} was performed with an ultra-fast Look-Locker echo-planar imaging T1 mapping sequence (26).

Two additional image acquisitions, one three-dimensional (3D) and one 2D, were acquired to aid in multi-subject registration. First, a high-resolution whole brain T1-weighted 3D image was acquired for each subject using MPRAGE (Magnetization Prepared Rapid Acquisition with Gradient-Echo imaging), with the following settings: 160 sagittal slices with field of view (FOV) = 256 × 256 mm^2; voxel size = 1 × 1 × 1 mm^3; TR = 1500 ms; TI = 800 ms; TE = 2.83 ms; flip angle 15 degrees; and one average. Next, a 2D T1-weighted image was acquired during each MR session using the same slice positions as the perfusion-weighted images and the following additional settings: FOV = 256 × 256 mm^2; in-plane resolution 1 × 1 mm^2; TR = 300 ms; TE = 3.69 ms; flip angle 60 degrees; and two averages.

Data Processing

Intra-subject Motion Correction, Perfusion- and BOLD-Weighted Images—

Perfusion-weighted and the proton-density weighted images were motion-corrected using the Statistical Parametric Mapping package (SPM99), by means of a six-parameter rigid-body transformation. The mean image of the motion-corrected proton density images was used for CBF mapping. Time series of the perfusion-weighted images were then obtained by pair-wise "surround" subtraction between interleaved label and control pairs (27–29) for each resting and activated condition during anesthesia or anesthesia-free sessions. The BOLD weighted images were derived by adding each label/control pair. The mean perfusion- and BOLD-weighted images were calculated for each condition.

Inter-subject Integration—

The mean perfusion-weighted image for each condition was used to estimate the map of absolute CBF. The following parameters were used in calculating the absolute CBF map: a longitudinal relaxation time for arterial blood of T_{1a}=1490 ms; a tissue blood partition coefficient for water of $\lambda = 0.9\ g^{-1}/mL^{-1}$; an RF labeling efficiency of α_π = 0.95; and a postlabeling delay time for the first slice of *TI* = 1400 ms (30). For each subject, maps of task-induced differences in CBF or BOLD were obtained by contrasting all measurements for the two conditions (e.g., visual vs rest). A standard whole brain template (MNI-1mm) was used for subject spatial normalization of the individual data. Subject registration was carried out using the BioImageSuite software package (31) for maps of task-induced changes in the CBF or BOLD values. Two transformations were calculated and used in multiple subject integration: (i) an affine transformation was estimated by co-registering the 2D anatomical image to the high-resolution 3D anatomical image of each individual, and this was then used to transform the individual maps of task-induced changes in CBF or BOLD to the high-resolution 3D anatomical space of that subject; (ii) a nonlinear transformation was used to co-register the high-resolution 3D anatomical image of each individual to the brain template, which enabled warping of all the transformed maps of an individual subject from step (i) to a common brain space. Tri-linear interpolation was used for image re-gridding. The mean, standard deviation, and statistics were estimated in the common template space on the

pooled-subject data. In summary, first, the individual maps of task-induced changes in CBF or BOLD were estimated and then transformed to the common reference brain space; and second, voxel-wise contrasts between conditions were estimated in the common space on the pooled-subject data using a t-statistic to test the null hypothesis. Brain regions of interest were defined in the common reference space based on the BOLD t-statistic map in the anesthesia-free condition (see Fig. 1a, top), corrected for multiple-voxel comparisons. Bonferroni correction for multiple voxel comparisons was used in the definition of the auditory and visual regions of interest (ROIs): the per-voxel t-statistics were first calculated on the pooled-subject data and then thresholded with P_{vox} to obtain a corrected threshold of $p = p_{vox} \cdot V_{roi} < 0.05$ (where V_{roi} is the size of the ROI considered) (32–36).

We first examined task-induced changes in both BOLD and CBF for the anesthesia-free and anesthesia conditions. Within the visual and auditory ROIs defined, the effect of sevoflurane on baseline CBF and the changes in CBF were evaluated; the coupling between task-induced changes in CBF and BOLD was assessed using analysis of covariance (ANCOVA) and multiple-comparison procedures for the different conditions (37).

RESULTS

After administration of 0.25 MAC sevoflurane, physiological parameters such as end-tidal CO_2, heart rate, and mean blood pressure were not significantly altered relative to the anesthesia-free state, as shown in Table 1. The anesthetic effects of 0.25 MAC sevoflurane on the task-induced changes in BOLD and regional CBF are demonstrated in Figure 1. The t-values shown in Figure 1 were calculated on the pooled-subject task-induced differences.

ASL measurements not only provided an index of task-induced differences under the different conditions, as displayed in Figure 1, but also provided an absolute baseline CBF. This made it possible to evaluate the effects of low-dose sevoflurane on both baseline CBF and the task-induced differences in CBF, as displayed in Figure 2 for both visual and auditory ROIs. In the visual ROI, the baseline CBF measured was 37.4 ± 4.2 and 33.1 ± 4.7 mL/100 g/min with and without anesthesia; the task-induced changes in CBF were 10.5 ± 2.6 and 5.0 ± 3.0 mL/100 g/min, respectively. In the auditory ROI, the baseline CBF was 45.4 ± 3.6 and 43.3 ± 4.4 mL/100 g/min with and without anesthesia; the task-induced changes in CBF were 4.9 ± 1.7 and 3.3 ± 3.0 mL/100 g/min, respectively.

Because BOLD and CBF were simultaneously measured in our study, we can evaluate the effect of sevoflurane on the regional coupling of flow as indexed by CBF and oxygenation as indexed by BOLD. We used ANCOVA in analysis of the CBF-BOLD coupling with the basic assumption that within each ROI, the task-induced changes in CBF and BOLD were within the linear regime of the BOLD-CBF coupling relationship (38). This assumption was validated by simulation showing a linear relationship over the range of the data addressed in this study (Fig. 5).

Each voxel is associated with the task-induced changes in both CBF and BOLD (abbreviated ΔCBF and ΔBOLD) under certain conditions, that is, anesthesia or anesthesia-free. The 2D XY scatter plots in Figure 3a represent the voxel-wise ΔCBF and ΔBOLD within the visual ROI during the anesthesia-free (blue) and anesthesia (green) conditions. The linear regression lines in Figure 3a show the dependence of ΔBOLD on ΔCBF within that ROI – in other words, they show the coupling between task-induced changes in BOLD and CBF in the anesthesia-free and anesthesia conditions. By using ΔBOLD as the response variable and ΔCBF as a covariate in the ANCOVA model, the analysis revealed that ΔBOLD was significantly affected by sevoflurane after ΔCBF was taken into account ($P < 0.001$). As to the BOLD-CBF coupling captured by the regression lines, the multiple comparison procedures showed that both the

slope and intercept of the regression line were significantly altered by sevoflurane ($P < 0.0001$). Figure 3b displays an analysis similar to that in Figure 3a, except rather than displaying relationships between absolute values of ΔCBF and ΔBOLD it displays relative values, that is, ΔCBF/CBF and ΔBOLD/BOLD (see Fig. 3 legend for details). The ANCOVA analysis showed that the task-induced relative change in ΔBOLD was significantly affected by sevoflurane ($P < 0.005$). As to the BOLD-CBF coupling captured by the regression lines, the multiple comparison procedures showed that both the slope and intercept of the regression line were significantly altered by sevoflurane ($P < 0.001$).

Similar data analysis procedures were repeated for the auditory ROI and the results are presented in Figure 4a,b. In summary, the following results were found for both absolute and relative BOLD and CBF changes: (i) the task-induced change in BOLD was significantly affected by sevoflurane after the change in CBF was taken into account ($P < 0.001$); (ii) both the slope and intercept of the regression line of the absolute BOLD-CBF coupling were significantly altered by sevoflurane ($P < 0.0001$), and (iii) both the slope and intercept of the regression line of the relative BOLD-CBF coupling were significantly altered by sevoflurane ($P < 0.0001$).

To examine whether BOLD-CBF coupling varies between auditory and visual ROIs, inter-regional comparisons of the BOLD-CBF coupling relationship were carried out for anesthesia-free and anesthesia conditions. For both absolute and relative changes, the slopes and intercepts of the regression lines were significantly different between ROIs for both the anesthesia-free condition ($P < 0.0001$) and the anesthesia condition ($P < 0.0001$).

DISCUSSION

Low-dose sevoflurane significantly depressed resting-state baseline CBF and the task-induced CBF changes in both the auditory and visual ROIs. Sevoflurane decreased the slopes of regression lines in both the visual and auditory ROIs, which suggested that sevoflurane changes the task-induced CBF-BOLD coupling. Indeed, for both ROIs examined a unit change in CBF was associated with a greater change in BOLD during anesthesia than in the absence of sevoflurane.

In the auditory ROI, administration of the agent caused a decrease in the goodness of fit measure (see changes in R-values in Fig. 4), indicating greater uncertainty in the CBF-BOLD coupling in this region during anesthesia. Although we do not know the cause of this observation, it might be related to variability in each individual's physiologic response to the agent.

Inter-regional comparisons showed that the task-induced CBF-BOLD coupling was region-specific, and this coupling was affected by sevoflurane.

Ambiguity in fMRI Data Interpretation in the Presence of an Anesthetic

In Figure 3a, the same observed change in CBF, f_1, brings about different changes in the tissue oxygenation, b_1 and b_2, for the anesthesia-free and anesthetized conditions, respectively. Similarly, a single change in tissue oxygenation, b_2, corresponds to different changes in CBF, f_1 and f_2, for the anesthesia-free and anesthetized conditions, respectively. Because the sevoflurane altered the coupling, neither the change in CBF nor the change in BOLD alone could be used to unambiguously infer the change in oxidative metabolism or neuronal activity in the presence of sevoflurane.

Regional CBF, CBV, BOLD, and Quantitative fMRI

Inferring neuronal activity and metabolism based on the MR-measured vascular changes (e.g., CBF and CBV) and BOLD is the goal of quantitative fMRI. Establishing the link between

BOLD signal changes and a more solid index of neuronal activity such as neuronal metabolism has been an area of active research for some time (38–42). Given that the BOLD signal is an epi-phenomenon—a result of the complex interplay between neurophysiologic processes involving oxygen supply, oxygen consumption, and the vascular system – interpreting quantitative fMRI has turned out to be a formidable task, especially in cases where a drug may be involved (10). That the task-induced CBF-BOLD coupling is significantly affected by an anesthetic indicates that quantitative fMRI models must be calibrated under the same anesthetic conditions as the testing that will be undertaken. The regional dependence of the change in coupling between the awake and anesthetic conditions suggests that the calibration in one region cannot necessarily be applied to any other brain region. Such calibration may also be dose-specific as differential flow effects have been observed at different dose levels (43,44).

To obtain more insight into the possible sources that caused the observed changes in this study, data were simulated using an fMRI quantitative model (39) with the following parameters: $\alpha = 0.38$, $\beta = 1.5$, and $M = 0.08$. Consistent with our experimental observations, the simulation data, shown in Figure 5, indicate that a decrease in α, or an increase in β and/or M, will decrease the slope of the BOLD-CBF coupling. If the parameters of the fMRI model were not affected by sevoflurane, that is, the model or all related couplings remained constant, the mean relative CMRO2 in the visual ROI would be 0.13 in the awake condition, and drop to 0.06 during anesthesia; in the auditory ROI it changed from 0.028 to 0.013. During anesthesia, however, a decrease in α is very probable, because any increase in the vascular occupancy or CBV, as a result of the vasodilative effect of sevoflurane, likely alters the vaso-reactivity. Let us suppose sevoflurane altered the CBV-CBF coupling such that α was changed from 0.38 to 0.1 for example, then during anesthesia the mean relative CMRO2 would be 0.095 for the visual task and 0.02 for auditory. But the iso-CMRO2 lines shown in Figure 5 indicate that increases in α alone cause only a small decrease in the slope of the regression line, which is not as large a change as observed in this study. Changes in β and/or M are also possible. It should be noted that α, β, and M are interdependent (39). Any increase in baseline CBV or β will increase M, while any increase in β or M further decrease the slope of the regression lines. It is very likely that the slope change in the slopes of the regression lines observed in this study resulted from a combination of changes in all these three parameters. One-parameter calibration procedure is simply not enough for the quantitative fMRI model to appreciate oxygen consumption in the presence of drugs.

In most quantitative fMRI practices, two model parameters, α and β, are often borrowed from the previous studies (45,46) and assumed to be global constants; M is calibrated; and $\Delta CBF/CBF$ and $\Delta BOLD/BOLD$ are measured. The constant α, for example, indicates unaltered CBF-CBV coupling, which is unlikely in cases where a drug is involved. For cases where the CBF-CBV coupling is altered by a drug, two models should be used: one for the case when the drug is present and the other in the drug-free situation. A handful of recent studies raised additional issues with respect to the use of CO2 for model calibration. It has been demonstrated that a significant source of regional variability arises when using hypercapnia for calibration; incorrect calibrated parameters obviously then propagate error into the rest of the experiment (47,48). The coupling relationship has also previously been shown to be time-varying and stimulus-dependent (49,50).

We cannot directly compare our results with previous observations (5,7,9) in terms of task-induced changes in CBF or BOLD with and without anesthesia. In general, our findings are not consistent with those animal studies however the studies differ on many dimensions. These include differences in the neurophysiology of the human and rate brain, the anesthetic agents applied, the doses, the lack of an awake condition in the animal studies, the type of stimuli applied and its intensity, in addition to the methodology used to calibrate the models.

Some recently studies on neurovascular coupling showed that vascular changes were altered and they were unnecessarily coupled to neuronal activity in the presence of a large variety of drugs. Dutka et al. investigated changes in task-induced CBF-BOLD coupling in rats before and after multiple exposures of transient hypercapnia (51). During hypercapnia exposures, the baseline CBF increased progressively over time with a trend of increasing significance, whereas the baseline BOLD quickly reached a plateau and the increase was not significant. They also found that the task-induced changes in CBF increased progressively after each exposure and the changes were signifi-cant; while the task-induced changes in BOLD were approximately the same after all three transient hypercapnia exposures and none of them are significant compared with the control. Duong et al. used O_2 and CO_2 as chemical stimulants to elicit CBF and BOLD changes in rats which were either awake or anesthetized by isoflurane (52,53). They found isoflurane attenuated autonomic responses to hypoxia, hypoxia-induced hypocapnia dominated CBF changes, tissues in awake conditions were better oxygenated, and severe hypoxia reduced oxygen metabolism. Their observations suggested marked differences in the BOLD and CBF responses to hypoxia between the awake and anesthetized conditions. In their hypocapnia study, substantially higher BOLD and CBF responses were observed under the awake condition, suggesting that cerebrovascular reactivity was suppressed by the anesthetic agent. In a study done by Liu et al., BOLD responses elicited by a visual stimulus showed distinct characteristics between transit-state and steady-state hypercapnia in normal subjects (54). In rats anesthetized by different anesthetic agents, the coupling between stimulated BOLD and local field potential recordings remained linear; however, the slopes of the regression lines were dependent on the particular anesthetic used—urethane or α-chloralose (55). BOLD increases during hypercapnia were investigated during remifentanil administration and in general remifentanil did not have obvious effects on CO_2 responsiveness in the cerebral vasculature (56) in human. Regional variations of neurovascular coupling were also inspected recently (47,57) in anesthetized rats, and field potentials and changes in CBF evoked by typical forepaw stimulation were measured. Under 1 MAC isoflurane the field potential and BOLD changes were markedly less than under α-chloralose (45 mg/kg/h) and the relative amplitudes of these changes depended on the stimulation parameters (58), suggesting that different anesthetics affect the field potential and CBF responses in different manners. In general there appears to be a growing consensus suggesting an altered coupling relationship across a large variety of agents.

Some Methodological Considerations

Physiological and physical limits on the number of slices for each radio frequency labeling make whole brain coverage difficult (59–61). In a recent study (62), single slice PASL MRI measurements were performed as a function of in-plane spatial resolution and postlabeling delay, and their results indicated that, when using postlabeling delays shorter than 1500 ms, higher MRI gray matter flow values may be observed owing to signal contamination from the remaining arterial blood water label. For delays above 1500 ms, regional PASL-based CBF values from frontal gray matter and occipital gray matter were comparable with PET-based measurements which can be obtained by using spatial resolutions comparable with PET (5−7.5 mm in-plane). At high resolution ($2.5 \times 2.5 \times 3mm^3$), compared with that at low resolution ($7.5 \times 7.5 \times 3mm^3$), gray matter CBF values were found to increase by 10−20%, and this difference was attributed to a reduction in partial volume effects. To obtained full coverage of the visual and auditory cortices, the slice thickness was set to 8 mm, with 2 mm gap between slices. A calculation based on the voxel sizes suggests that an 8−16% underestimation for CBF is possible with this resolution. Some of the disadvantages of ASL imaging include low signal-to-noise ratio (63), contamination from the intravascular signal (64), variability of the arterial transit time (65–67), and physiological and physical limits on the number of slices for each radio frequency (RF) label. Recently Woolrich et al. (68) modeled the double-echo ASL process using a general linear model and a Bayesian statistical inference model. Their data

indicate that the fractional change in BOLD obtained by averaging tag/control pairs from a single-echo ASL experiment could be underestimated by up to 25%. This underestimation is caused by the residual signal components of static magnetization from the labeled or unlabeled blood. Because in this study, we focused on the anesthetic effects on the task-induced CBF-BOLD coupling, relative to the anesthesia-free condition, the bias in CBF or BOLD measurement will unlikely affect our observation if it is present similarly with or without anesthesia. Further studies are required to clarify these issues.

CONCLUSIONS

Low-dose sevoflurane decreased the task-induced incremental changes in both BOLD and CBF. Within the visual and auditory ROIs, both baseline CBF and the task-induced changes in CBF decreased significantly when the brain was challenged by low-dose sevoflurane. When the task-induced changes in both CBF and BOLD were considered, low-dose sevoflurane significantly altered the task-induced CBF-BOLD coupling in spatially nonuniform manner. Compared with the anesthesia-free condition, a larger change in BOLD was observed per unit change of CBF during anesthesia. The alteration of task-induced CBF-BOLD coupling by an anesthetic must be taken into consideration when examining BOLD effects in the presence of an anesthetic agent (or potentially any other medication). The coupling between neuronal activity, metabolism, CBF, and BOLD is dependent on many factors and an anesthetic agent may impact this coupling by altering any of these factors, suggesting that careful calibration in the appropriate brain region and at the does of interest is needed for accurate quantitative fMRI. That is, spatially variable cortical responses to anesthetic agents in terms of their effects on the coupling between BOLD and CBF changes, require that calibration be performed on the specific cortical region of interest and that calibration in a specific region can not be generalized to whole brain quantitative fMRI.

ACKNOWLEDGMENTS

We are grateful to Dr. Fahmeed Hyder (Yale University), Dr. Robert G. Shulman (Yale University) for their insightful suggestions, as well as Dr. Jiongjiong Wang (University of Pennsylvania for discussions on ASL CBF Measurements. We also thank Karen Martin, Hedy Sarofin, and Terry Hickley for their assistance with data collection.

REFERENCES

1. Fox PT, Raichle ME. Focal physiological uncoupling of cerebral blood flow and oxidative metabolism during somatosensory stimulation in human subjects. Proc Natl Acad Sci U S A 1986;83:1140–1144. [PubMed: 3485282]
2. Fox PT, Raichle ME, Mintun MA, Dence C. Nonoxidative glucose consumption during focal physiologic neural activity. Science 1988;241:462–464. [PubMed: 3260686]
3. Ogawa S, Lee TM, Kay AR, Tank DW. Brain magnetic resonance imaging with contrast dependent on blood oxygenation. Proc Natl Acad Sci U S A 1990;87:9868–9872. [PubMed: 2124706]
4. Ogawa S, Menon RS, Tank DW, Kim SG, Merkle H, Ellermann JM, Ugurbil K. Functional brain mapping by blood oxygenation level-dependent contrast magnetic resonance imaging. A comparison of signal characteristics with a biophysical model. Biophys J 1993;64:803–812. [PubMed: 8386018]
5. Hyder F, Rothman DL, Shulman RG. Total neuroenergetics support localized brain activity: implications for the interpretation of fMRI. Proc Natl Acad Sci U S A 2002;99:10771–10776. [PubMed: 12134057]
6. Shulman RG, Hyder F, Rothman DL. Cerebral energetics and the glycogen shunt: neurochemical basis of functional imaging. Proc Natl Acad Sci U S A 2001;98:6417–6422. [PubMed: 11344262]
7. Shulman RG, Hyder F, Rothman DL. Biophysical basis of brain activity: implications for neuroimaging. Q Rev Biophys 2002;35:287–325. [PubMed: 12599751]
8. Shulman RG, Rothman DL, Hyder F. Stimulated changes in localized cerebral energy consumption under anesthesia. Proc Natl Acad Sci U S A 1999;96:3245–3250. [PubMed: 10077669]

9. Sibson NR, Shen J, Mason GF, Rothman DL, Behar KL, Shulman RG. Functional energy metabolism: in vivo 13C-NMR spectroscopy evidence for coupling of cerebral glucose consumption and glutamatergic neuronalactivity. Dev Neurosci 1998;20:321–330. [PubMed: 9778568]
10. Austin VC, Blamire AM, Allers KA, Sharp T, Styles P, Matthews PM, Sibson NR. Confounding effects of anesthesia on functional activation in rodent brain: a study of halothane and alpha-chloralose anesthesia. Neuroimage 2005;24:92–100. [PubMed: 15588600]
11. Salmi E, Kaisti KK, Metsahonkala L, Oikonen V, Aalto S, Nagren K, Hinkka S, Hietala J, Korpi ER, Scheinin H. Sevoflurane and propofol increase 11C-flumazenil binding to gamma-aminobutyric acidA receptors in humans. Anesth Analg 2004;99:1420–1426. [PubMed: 15502041]Table of contents
12. Kira T, Harata N, Sakata T, Akaike N. Kinetics of sevoflurane action on GABA- and glycine-induced currents in acutely dissociated rat hippocampal neurons. Neuroscience 1998;85:383–394. [PubMed: 9622238]
13. Franks NP. Molecular targets underlying general anaesthesia. British journal of pharmacology 2006;147(Suppl 1):S72–S81. [PubMed: 16402123]
14. Franks NP, Lieb WR. Which molecular targets are most relevant to general anaesthesia? Toxicol Lett 1998;100−101:1–8.
15. Orser BA, Canning KJ, Macdonald JF. Mechanisms of general anesthesia. Curr Opin Anaesthesiol 2002;15:427–433. [PubMed: 17019234]
16. Wu J, Harata N, Akaike N. Potentiation by sevoflurane of the gamma-aminobutyric acid-induced chloride current in acutely dissociated CA1 pyramidal neurones from rat hippocampus. Br J Pharmacol 1996;119:1013–1021. [PubMed: 8922750]
17. Wang YW, Deng XM, You XM, Liu SX, Zhao ZQ. Involvement of GABA and opioid peptide receptors in sevoflurane-induced antinociception in rat spinal cord. Acta Pharmacol Sin 2005;26:1045–1048. [PubMed: 16115369]
18. Moe MC, Berg-Johnsen J, Larsen GA, Roste GK, Vinje ML. Sevoflurane reduces synaptic glutamate release in human synaptosomes. J Neurosurg Anesthesiol 2002;14:180–186. [PubMed: 12172289]
19. Vinje ML, Moe MC, Valo ET, Berg-Johnsen J. The effect of sevoflurane on glutamate release and uptake in rat cerebrocortical presynaptic terminals. Acta Anaesthesiol Scand 2002;46:103–108. [PubMed: 11903082]
20. Grasshoff C, Antkowiak B. Propofol and sevoflurane depress spinal neurons in vitro via different molecular targets. Anesthesiology 2004;101:1167–1176. [PubMed: 15505453]
21. Franks NP, Lieb WR. Molecular and cellular mechanisms of general anaesthesia. Nature 1994;367:607–614. [PubMed: 7509043]
22. Silva JH, Gomez RS, Diniz PH, Gomez MV, Guatimosim C. The effect of sevoflurane on the release of [3H]dopamine from rat brain cortical slices. Brain Res Bull 2007;72:309–314. [PubMed: 17452291]
23. Edelman RR, Siewert B, Darby DG, Thangaraj V, Nobre AC, Mesulam MM, Warach S. Qualitative mapping of cerebral blood flow and functional localization with echo-planar MR imaging and signal targeting with alternating radio frequency. Radiology 1994;192:513–520. [PubMed: 8029425]
24. Wong EC, Buxton RB, Frank LR. Quantitative imaging of perfusion using a single subtraction (QUIPSS and QUIPSS II). Magn Reson Med 1998;39:702–708. [PubMed: 9581600]
25. Luh WM, Wong EC, Bandettini PA, Hyde JS. QUIPSS II with thin-slice TI1 periodic saturation: a method for improving accuracy of quantitative perfusion imaging using pulsed arterial spin labeling. Magn Reson Med 1999;41:1246–1254. [PubMed: 10371458]
26. Freeman AJ, Gowland PA, Mansfield P. Optimization of the ultrafast Look-Locker echo-planar imaging T1 mapping sequence. Magn Reson Imaging 1998;16:765–772. [PubMed: 9811142]
27. Aguirre GK, Detre JA, Zarahn E, Alsop DC. Experimental design and the relative sensitivity of BOLD and perfusion fMRI. Neuroimage 2002;15:488–500. [PubMed: 11848692]
28. Wong EC, Buxton RB, Frank LR. Implementation of quantitative perfusion imaging techniques for functional brain mapping using pulsed arterial spin labeling. NMR Biomed 1997;10:237–249. [PubMed: 9430354]
29. Wang J, Aguirre GK, Kimberg DY, Roc AC, Li L, Detre JA. Arterial spin labeling perfusion fMRI with very low task frequency. Magn Reson Med 2003;49:796–802. [PubMed: 12704760]

30. Yang Y, Gu H, Silbersweig DA, Stern E. Simultaneous perfusion and blood-oxygenation-level-dependent measurements using single-shot interleaved z-shim echo-planar imaging. Magn Reson Med 2005;53:1207–1211. [PubMed: 15844153]

31. Papademetris X, Jackowski AP, Schultz RT, Staib LH, Duncan JS. Integrated intensity and point-feature nonrigid registration. Med Image Comput Comput Assist Interv Int Conf Med Image Comput Comput Assist Interv 2004;3216:763–770.

32. Marcar VL, Girard F, Rinkel Y, Schneider JF, Martin E. Inaudible functional MRI using a truly mute gradient echo sequence. Neuroradiology 2002;44:893–899. [PubMed: 12428122]

33. Siegle GJ, Carter CS, Thase ME. Use of FMRI to predict recovery from unipolar depression with cognitive behavior therapy. Am J Psychiatry 2006;163:735–738. [PubMed: 16585452]

34. Wilkinson ID, Romanowski CA, Jellinek DA, Morris J, Griffiths PD. Motor functional MRI for pre-operative and intraoperative neurosurgical guidance. Br J Radiol 2003;76:98–103. [PubMed: 12642277]

35. O'Craven KM, Rosen BR, Kwong KK, Treisman A, Savoy RL. Voluntary attention modulates fMRI activity in human MT-MST. Neuron 1997;18:591–598. [PubMed: 9136768]

36. D'Esposito M, Postle BR, Jonides J, Smith EE. The neural substrate and temporal dynamics of interference effects in working memory as revealed by event-related functional MRI. Proc Natl Acad Sci U S A 1999;96:7514–7519. [PubMed: 10377446]

37. Hochberg, Y.; Tamhane, AC. Multiple comparison procedures. Vol. xxii. Wiley; New York: 1987. p. 450

38. Hoge RD, Atkinson J, Gill B, Crelier GR, Marrett S, Pike GB. Linear coupling between cerebral blood flow and oxygen consumption in activated human cortex. Proc Natl Acad Sci U S A 1999;96:9403–9408. [PubMed: 10430955]

39. Hoge RD, Atkinson J, Gill B, Crelier GR, Marrett S, Pike GB. Investigation of BOLD signal dependence on cerebral blood flow and oxygen consumption: the deoxyhemoglobin dilution model. Magn Reson Med 1999;42:849–863. [PubMed: 10542343]

40. Hyder F, Kida I, Behar KL, Kennan RP, Maciejewski PK, Rothman DL. Quantitative functional imaging of the brain: towards mapping neuronal activity by BOLD fMRI. NMR Biomed 2001;14:413–431. [PubMed: 11746934]

41. Kim SG. Quantification of relative cerebral blood flow change by flow-sensitive alternating inversion recovery (FAIR) technique: application to functional mapping. Magn Reson Med 1995;34:293–301. [PubMed: 7500865]

42. Kim SG, Rostrup E, Larsson HB, Ogawa S, Paulson OB. Determination of relative CMRO2 from CBF and BOLD changes: significant increase of oxygen consumption rate during visual stimulation. Magn Reson Med 1999;41:1152–1161. [PubMed: 10371447]

43. Kaisti KK, Langsjo JW, Aalto S, Oikonen V, Sipila H, Teras M, Hinkka S, Metsahonkala L, Scheinin H. Effects of sevoflurane, propofol, and adjunct nitrous oxide on regional cerebral blood flow, oxygen consumption, and blood volume in humans. Anesthesiology 2003;99:603–613. [PubMed: 12960544]

44. Kaisti KK, Metsahonkala L, Teras M, Oikonen V, Aalto S, Jaaskelainen S, Hinkka S, Scheinin H. Effects of surgical levels of propofol and sevoflurane anesthesia on cerebral blood flow in healthy subjects studied with positron emission tomography. Anesthesiology 2002;96:1358–1370. [PubMed: 12170048]

45. Grubb RL Jr, Raichle ME, Eichling JO, Ter-Pogossian MM. The effects of changes in PaCO2 on cerebral blood volume, blood flow, and vascular mean transit time. Stroke 1974;5:630–639. [PubMed: 4472361]

46. Boxerman JL, Bandettini PA, Kwong KK, Baker JR, Davis TL, Rosen BR, Weisskoff RM. The intravascular contribution to fMRI signal change: Monte Carlo modeling and diffusion-weighted studies in vivo. Magn Reson Med 1995;34:4–10. [PubMed: 7674897]

47. Chiarelli PA, Bulte DP, Gallichan D, Piechnik SK, Wise R, Jezzard P. Flow-metabolism coupling in human visual, motor, and supplementary motor areas assessed by magnetic resonance imaging. Magn Reson Med 2007;57:538–547. [PubMed: 17326178]

48. Chiarelli PA, Bulte DP, Piechnik S, Jezzard P. Sources of systematic bias in hypercapnia-calibrated functional MRI estimation of oxygen metabolism. Neuroimage 2007;34:35–43. [PubMed: 17029987]

49. Kida I, Rothman DL, Hyder F. Dynamics of changes in blood flow, volume, and oxygenation: implications for dynamic functional magnetic resonance imaging calibration. J Cereb Blood Flow Metab 2007;27:690–696. [PubMed: 17033688]
50. Ances BM, Zarahn E, Greenberg JH, Detre JA. Coupling of neural activation to blood flow in the somatosensory cortex of rats is time-intensity separable, but not linear. J Cereb Blood Flow Metab 2000;20:921–930. [PubMed: 10894175]
51. Dutka MV, Scanley BE, Does MD, Gore JC. Changes in CBF-BOLD coupling detected by MRI during and after repeated transient hypercapnia in rat. Magn Reson Med 2002;48:262–270. [PubMed: 12210934]
52. Duong TQ. Cerebral blood flow and BOLD fMRI responses to hypoxia in awake and anesthetized rats. Brain Res 2007;1135:186–194. [PubMed: 17198686]
53. Sicard K, Shen Q, Brevard ME, Sullivan R, Ferris CF, King JA, Duong TQ. Regional cerebral blood flow and BOLD responses in conscious and anesthetized rats under basal and hypercapnic conditions: implications for functional MRI studies. J Cereb Blood Flow Metab 2003;23:472–481. [PubMed: 12679724]
54. Liu YJ, Juan CJ, Chen CY, Wang CY, Wu ML, Lo CP, Chou MC, Huang TY, Chang H, Chu CH, Li MH. Are the local blood oxygen level-dependent (BOLD) signals caused by neural stimulation response dependent on global BOLD signals induced by hypercapnia in the functional MR imaging experiment? Experiments of long-duration hypercapnia and multilevel carbon dioxide concentration. AJNR Am J Neuroradiol 2007;28:1009–1014. [PubMed: 17569947]
55. Huttunen JK, Grohn O, Penttonen M. Coupling between simultaneously recorded BOLD response and neuronal activity in the rat somatosensory cortex. Neuroimage 2008;39:775–785. [PubMed: 17964186]
56. Pattinson KT, Rogers R, Mayhew SD, Tracey I, Wise RG. Pharmacological FMRI: measuring opioid effects on the BOLD response to hypercapnia. J Cereb Blood Flow Metab 2007;27:414–423. [PubMed: 16736039]
57. Ances BM, Leontiev O, Perthen JE, Liang C, Lansing AE, Buxton RB. Regional differences in the coupling of cerebral blood flow and oxygen metabolism changes in response to activation: implications for BOLD-fMRI. Neuroimage 2008;39:1510–1521. [PubMed: 18164629]
58. Masamoto K, Kim T, Fukuda M, Wang P, Kim SG. Relationship between neural, vascular, and BOLD signals in isoflurane-anesthetized rat somatosensory cortex. Cereb Cortex 2007;17:942–950. [PubMed: 16731882]
59. Frank LR, Wong EC, Buxton RB. Slice profile effects in adiabatic inversion: application to multislice perfusion imaging. Magn Reson Med 1997;38:558–564. [PubMed: 9324322]
60. Yongbi MN, Yang Y, Frank JA, Duyn JH. Multislice perfusion imaging in human brain using the C-FOCI inversion pulse: comparison with hyperbolic secant. Magn Reson Med 1999;42:1098–1105. [PubMed: 10571931]
61. Campbell AM, Beaulieu C. Comparison of multislice and single-slice acquisitions for pulsed arterial spin labeling measurements of cerebral perfusion. Magn Reson Imaging 2006;24:869–876. [PubMed: 16916704]
62. Donahue MJ, Lu H, Jones CK, Pekar JJ, van Zijl PC. An account of the discrepancy between MRI and PET cerebral blood flow measures. A high-field MRI investigation. NMR Biomed 2006;19:1043–1054. [PubMed: 16948114]
63. Detre JA, Leigh JS, Williams DS, Koretsky AP. Perfusion imaging. Magn Reson Med 1992;23:37–45. [PubMed: 1734182]
64. Ye FQ, Mattay VS, Jezzard P, Frank JA, Weinberger DR, McLaughlin AC. Correction for vascular artifacts in cerebral blood flow values measured by using arterial spin tagging techniques. Magn Reson Med 1997;37:226–235. [PubMed: 9001147]
65. Gonzalez-At JB, Alsop DC, Detre JA. Cerebral perfusion and arterial transit time changes during task activation determined with continuous arterial spin labeling. Magn Reson Med 2000;43:739–746. [PubMed: 10800040]
66. Yang Y, Engelien W, Xu S, Gu H, Silbersweig DA, Stern E. Transit time, trailing time, and cerebral blood flow during brain activation: measurement using multislice, pulsed spin-labeling perfusion imaging. Magn Reson Med 2000;44:680–685. [PubMed: 11064401]

67. Zhou J, van Zijl PC. Effect of transit times on quantification of cerebral blood flow by the FAIR T (1)-difference approach. Magn Reson Med 1999;42:890–894. [PubMed: 10542347]

68. Woolrich MW, Chiarelli P, Gallichan D, Perthen J, Liu TT. Bayesian inference of hemodynamic changes in functional arterial spin labeling data. Magn Reson Med 2006;56:891–906. [PubMed: 16964610]

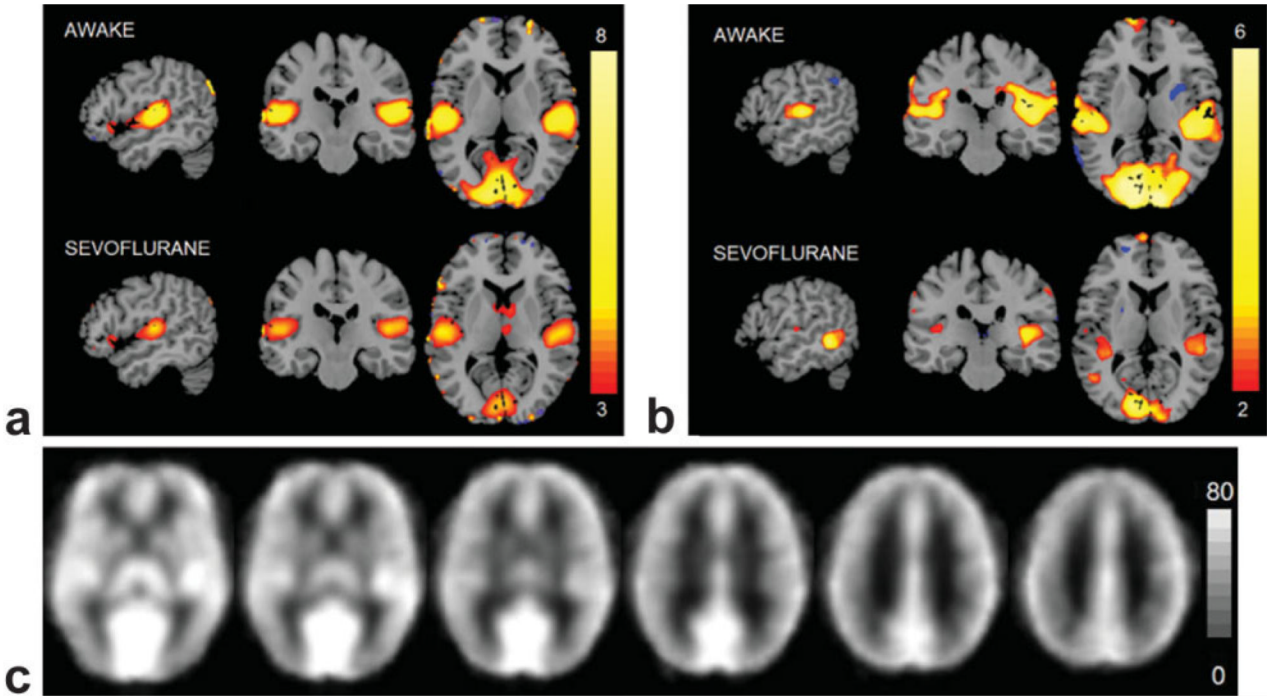

FIG. 1.

Changes in BOLD (a) and regional CBF (b) induced by the visual and auditory stimulations. The t-statistic was estimated on the pooled-subject data and is shown as a color bar on the right. **a:** BOLD activations are given for the sevoflurane-free (top) and anesthesia (bottom) conditions, respectively. **b:** Task-induced changes in CBF are demonstrated for the anesthesia-free condition (top), compared with those during anesthesia (bottom). **c:** Typical slices of the absolute regional CBF measured with ASL for the resting condition when no sevoflurane was given to the subjects (pooled-subject data); the gray scale is in mL/100 g/min.

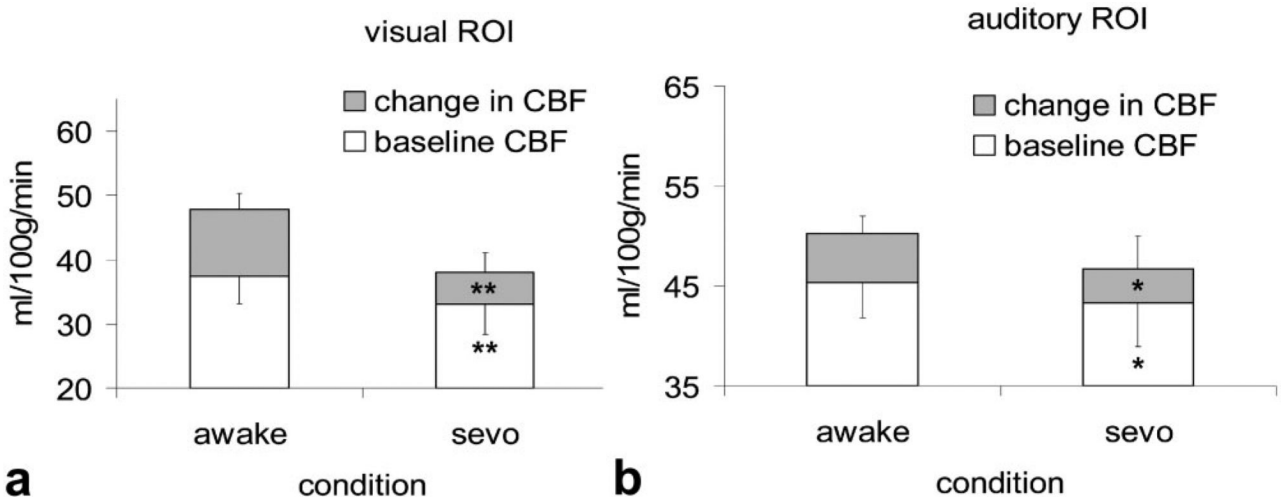

FIG. 2.

a,b: Resting-state baseline CBF and task-induced changes in CBF were estimated within the visual (a) and auditory (b) ROIs for the anesthesia-free and anesthesia conditions. Paired t-test per subjects was performed to evaluate the anesthetic effect on both resting state CBF and the task-induced changes. Asterisks show the significance (*$P < 0.05$; **$P < 0.01$) from the paired t-test for the resting state CBF values (white) and the task-induced changes (gray).

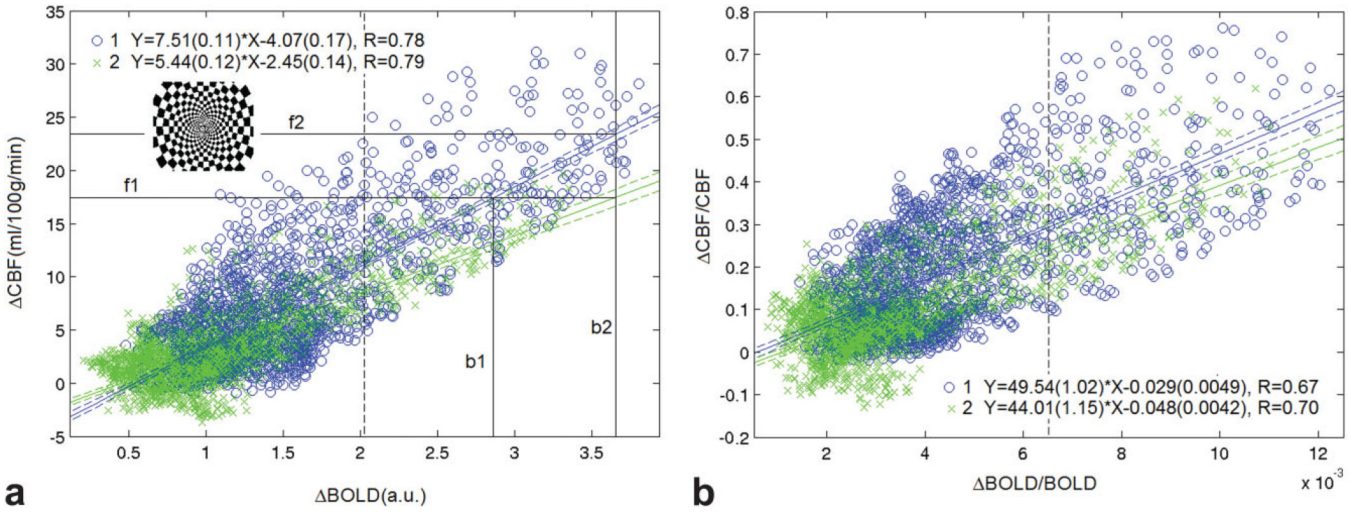

FIG. 3.

Regional CBF-BOLD coupling was assessed in the visual ROI in the anesthesia-free (blue O) and anesthesia (green X) conditions. A composite map representing visual task-induced changes in BOLD in the anesthesia-free condition was estimated on a per voxel basis on the pooled-subject data in the transformed common brain template space. The ROI was defined based on the composite map of task-induced BOLD changes and Bonferroni correction was applied for multiple voxel comparisons ($P < 0.01$). Within the visual ROI, each voxel is associated with the changes in both CBF and BOLD induced by the visual stimulus (inset), that is ΔCBF and ΔBOLD. Scatter plots are presented for the anesthesia-free and anesthesia conditions. **a:** The data are displayed as a collection of points, each representing the coordinated ΔCBF and ΔBOLD induced by the visual stimulus for one voxel within the ROI (*abscissa* ΔBOLD and ordinate ΔCBF). The prediction lines with 95% confidence bounds, the regression equations with estimates and their standard errors, and R-values for the goodness of fit are presented. **b:** Also estimated were relative changes in CBF and BOLD, calculated as ΔCBF/CBF and ΔBOLD/BOLD, where the denominator represents the baseline signal in the absence of stimuli.

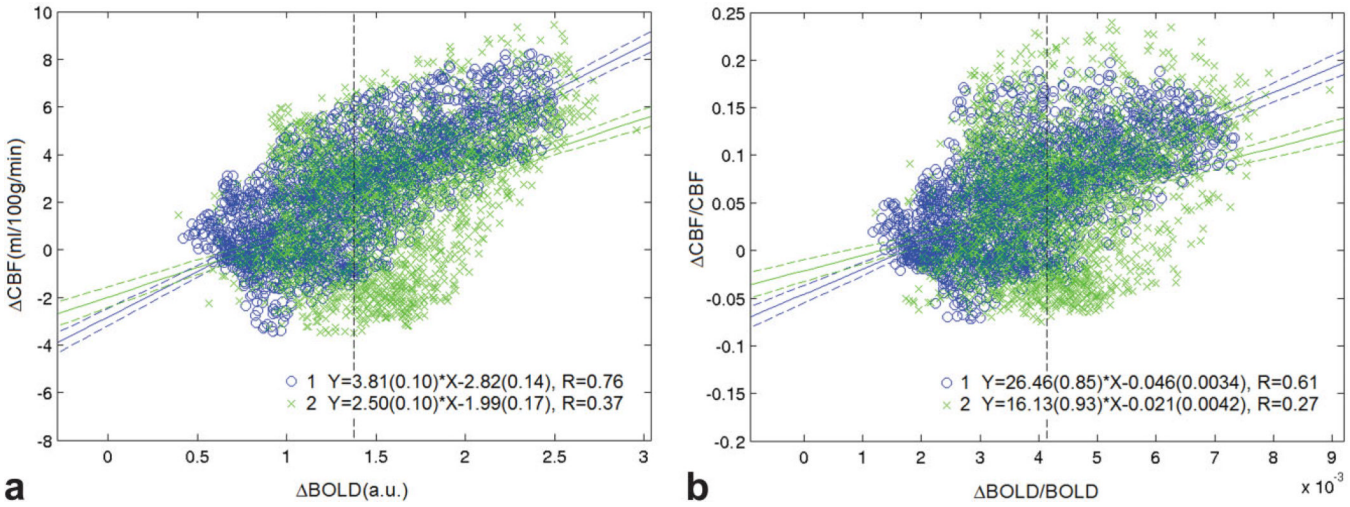

FIG. 4.

Regional CBF-BOLD coupling was assessed in the auditory ROI in the anesthesia-free (blue O) and anesthesia (green X) conditions. A composite map representing auditory task-induced changes in BOLD in the anesthesia-free condition was estimated on a per voxel basis on the pooled-subject data in the transformed common brain template space. The ROI was defined based on the composite map of task-induced BOLD changes and Bonferroni correction was applied for multiple voxel comparisons ($P < 0.01$). Within the auditory ROI, each voxel is associated with the changes in both CBF and BOLD induced by the auditory stimulus (see the Materials and Methods section), that is, ΔCBF and ΔBOLD. Scatter plots are presented for the anesthesia-free and anesthesia conditions. **a:** The data are displayed as a collection of points, each representing the coordinated ΔCBF and ΔBOLD induced by the auditory stimulus for one voxel within the ROI (*abscissa* ΔBOLD and *ordinate* ΔCBF). The prediction lines with 95% confidence bounds, the regression equations with estimates and their standard errors, and R-values for the goodness of fit are presented. **b:** Also estimated were relative changes in CBF and BOLD, calculated as ΔCBF/CBF and ΔBOLD/BOLD, where the denominator represents the baseline signal in the absence of stimuli.

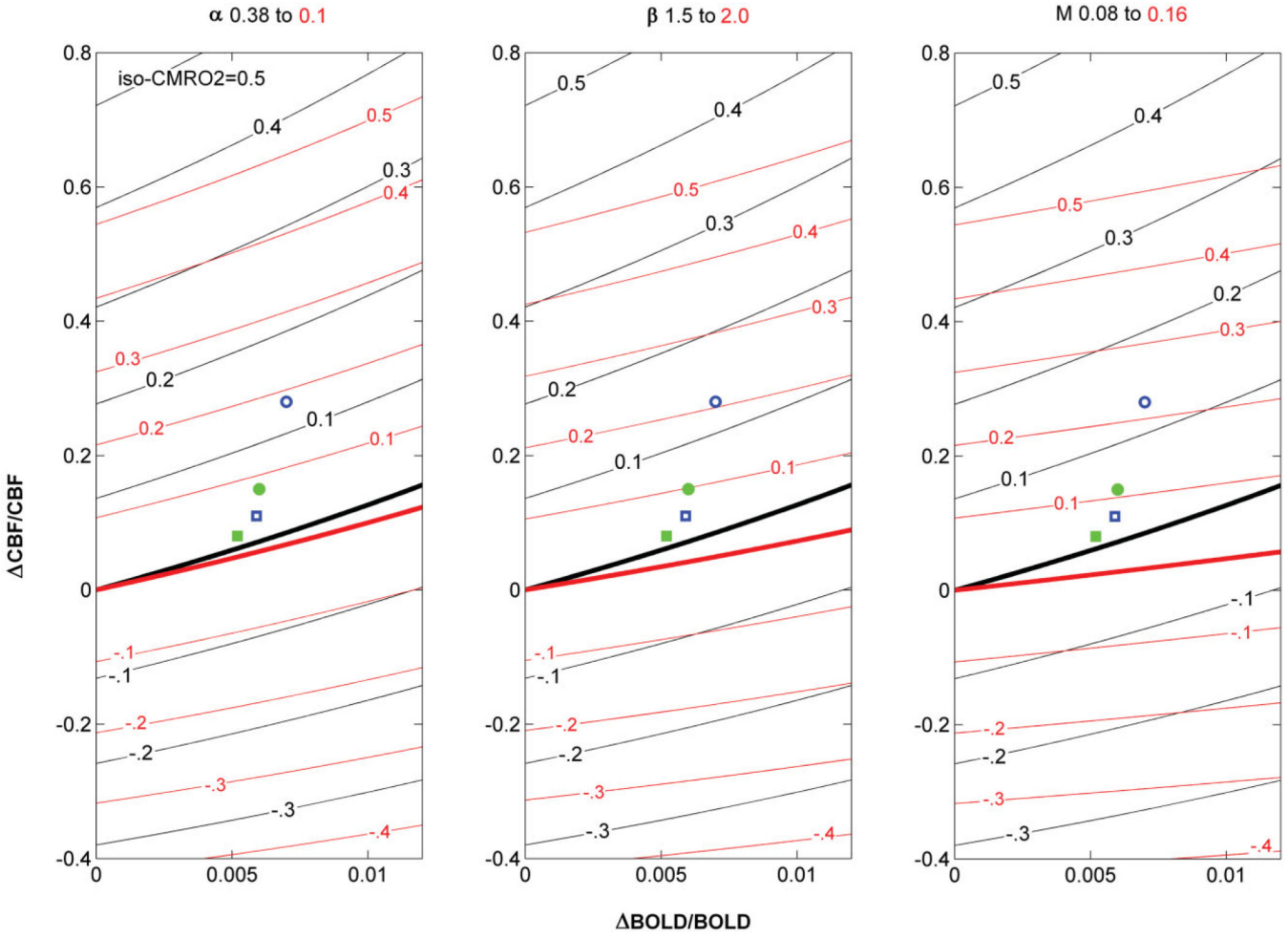

FIG. 5.

Data were simulated using an fMRI quantitative model (39) with the following default parameters: α = 0.38, β = 1.5, and M = 0.08. Mean task-induced relative changes in BOLD and CBF was plotted for two ROIs (visual marked by circles and auditory by squares) and for two conditions (awake by blue empty symbols and anesthesia by green solid). Iso-$CMRO_2$ curves (black) were calculated based on the default model parameters. When there is a change assumed in parameter α, β, or M, simulated iso-$CMRO_2$ curves are shown in red. The sign of the change in α, β, or M was chosen to decrease the slope of the regression line of BOLD-CBF coupling, as observed in this study. Because saturation of the BOLD signal causes nonlinearity of BOLD-CBF coupling and an increase in CMRO2 trends to reduce the saturation and thus the nonlinearity, the iso-CMRO2 lines give the upper limit of the nonlinearity. The parallel iso-$CMRO_2$ curves/lines validate our assumption that the task-induced changes in CBF and BOLD were within the linear regime of the BOLD-CBF coupling relationship.

Table 1

Physiological Parameters in the Anesthesia-Free and Anesthesia Conditions

Physiological measurements	**Sevoflurane-free**	**Sevoflurane**	***P* Value**
End-tidal CO_2, mmHg	36.3 ± 2.4	36.3 ± 2.7	0.98
Heart rate, beats/min	58.4 ± 4.8	58.2 ± 4.2	0.91
Mean blood pressure, mmHg	87.4 ± 6.7	85.9 ± 5.9	0.50